Polymer Chemistry

PAPER

View Article Online
View Journal | View Issue

Cite this: *Polym. Chem.*, 2016, **7**, 1569

Triphenylamine-based luminogens and fluorescent polyimides: effects of functional groups and substituents on photophysical behaviors†

Jia-Hao Wu, Wen-Chang Chen and Guey-Sheng Liou*

Received 5th December 2015,
Accepted 29th December 2015

DOI: 10.1039/c5py01939g

www.rsc.org/polymers

We prepared four series of triphenylamine (TPA)-based luminogens with various functional groups (diphthalic imide, tetracarboxylic acid, diphthalic anhydride, and pristine TPA) and substituted groups (–H, –Br, –CHO, and –CN), and corresponding fluorescent polyimides (PIs) were prepared from triarylamine-based dianhydride monomers with various aromatic and aliphatic diamine monomers for the investigation of their photophyscial behaviors. In the solution state, the introduction of strong electron acceptors such as formyl and cyano substituents in the luminogens induced strong emissions due to hybridized local and charge-transfer transitions (HLCTs). However, aggregated molecules containing these pendant electron-accepting groups resulted in quenching fluorescence behavior due to intermolecular interactions and energy transfers. Furthermore, the competition of aggregation-induced enhanced emission (AIEE) and aggregation-caused quenching (ACQ) effects was investigated and is discussed.

Introduction

Fluorescent materials have attracted significant academic and industrial interest for their numerous potential applications such as biosensors,[1] bio-imaging,[2] organic light-emitting diodes (OLEDs),[3] and other optoelectronic devices.[4] For most of these applications, fluorescent materials are often utilized in aggregated states with close interactions between their component molecules. However, most luminogens generally display partial or even complete quenching of light emission and a much lower photoluminescence quantum yield (PLQY) in the solid state than in solution, *i.e.*, the so-called aggregation-caused quenching (ACQ) effect. In 2001, a novel phenomenon of aggregation-induced emission (AIE) or aggregation-induced enhanced emission (AIEE), which was proposed by Tang *et al.*,[5] is exactly opposite to the ACQ effect, and provides for a new strategy for designing and synthesizing highly efficient luminogens in the aggregated state. In the past decade, many researchers have devoted their efforts to the interpretation of AIE mechanisms, in order to increase the understanding of luminescence processes and guide the design of new AIE luminogens.[6] A number of possible mechanistic pathways, including J-aggregate formation (JAF),[7] twisted intramolecular charge transfer (TICT),[8] excited-state intramolecular proton transfer (ESIPT),[9] and restriction of intramolecular motions (RIM),[10] have been proposed for the AIE phenomenon. Through a series of modulated experiments and theoretical studies, the RIM has been demonstrated as the main cause of the AIE effect for most AIE luminogens and polymers.[6a]

Triarylamine derivatives are well known for their photo- and electro-active properties and have potential for optoelectronic applications, such as photoconductors, hole transporters, light emitters, and memory devices.[11] The propeller-like structure and electron-donating characteristics of the triarylamine group make it a useful building block for the construction of AIE luminogens, and the emission colors can be tuned by prudently combining the triphenylamine (TPA) unit with various electron-accepting moieties. The photophysical behaviors of donor–acceptor (D–A) molecules based on various acceptors and TPA as the donor have been investigated by Yang and Ma.[12] Depending on the structure and environmental conditions, there are three possible causes for the first excited state (S_1) of these D–A molecules: (1) a locally excited (LE) π–π* transition, (2) a charge-transfer (CT) π–π* transition (a delocalized electronic state), and (3) a mixed or hybridized state of the LE and CT states called the hybridized local and charge-transfer (HLCT) state. A similarity of the energy levels of the LE and CT states would facilitate a high-efficiency mixing or hybridized HLCT state, and in such a case a strong

Institute of Polymer Science and Engineering, National Taiwan University, 1 Roosevelt Road, 4th Sec., Taipei 10617, Taiwan. E-mail: gsliou@ntu.edu.tw; Fax: +886-2-33665237; Tel: +886-2-33665315

† Electronic supplementary information (ESI) available: Table: inherent viscosity, molecular weights, solubility behavior, thermal, and optical properties. Figure: NMR, FT-IR, TGA, DSC, absorption spectra, photoluminescence spectra. See DOI: 10.1039/c5py01939g

emission can be expected. Recently, we reported new entirely aromatic and semi-aromatic AIEE-active triarylamine-containing polyimides (PIs) that exhibited high quantum efficiency values, respectively, of 22% and 32%, in the solid film state.[13] Fluorescent PIs based on central triarylamine dianhydrides with rigid phthalic imide structures have relatively extended conjugation and lower-energy band gaps, which result in the bathochromic shift of absorption and emission with high PLQYs displayed by these molecules in UV-Vis and PL spectra, respectively. On the other hand, the PIs based on a central triarylamine diamine have shown low PLQYs due to twist intramolecular charge transfer (TICT).

In the current work, in order to gain more insight into the fluorescent mechanism and photophysical behaviors of triarylamine-based luminogens and polyimides, we prepared four series of novel TPA-based luminogens with various functional groups (diphthalic imide, tetracarboxylic acid, diphthalic anhydride, and pristine TPA) and substituents (–H, –Br, –CHO, and –CN), and fluorescent polyimides (PIs) derived from their corresponding TPA-based dianhydride monomers with various aromatic and aliphatic diamine monomers. The UV-Vis absorption and PL spectra, as well as the molecular orbital transitions with density functional theory calculations of these TPA-based luminogens were extensively investigated. Moreover, the AIEE behavior of these obtained materials was also demonstrated by PL spectroscopy in the solution state with various fractions of poor solvent.

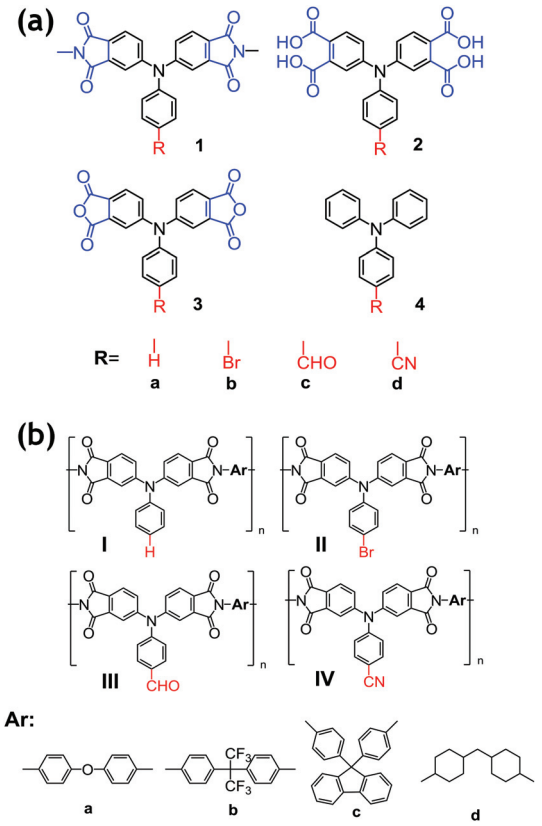

Scheme 1 The structures of the studied (a) small molecules and (b) polyimides.

Results and discussion

Monomer synthesis

The structures of the target materials are depicted in Scheme 1, and their synthetic routes are outlined in Schemes S1–S3.† The diimide compounds **1a**, **1c′** and **1d** were derived from double *N*-arylation reactions of primary amines with *N*-methyl-4-bromophthalimide and were carried out in the presence of palladium (II) acetate, *rac*-2,2′-bis(diphenylphosphino)-1,1′-binaphthyl (*rac*-BINAP), and cesium carbonate in toluene. Then, **1b** and **1c** were prepared, respectively, by bromination of **1a** with *N*-bromosuccinimide (NBS) and deprotection of **1c′** with *p*-toluenesulfonic acid (TsOH) in acetone/water. The **1a**, **1b** and **1c′** diimide compounds were then hydrolyzed with aqueous potassium hydroxide, giving the corresponding tetracarboxylic acids **2a**, **2b** and **2c**, which in turn were converted to the dianhydride monomers **3a**, **3b**, and **3c** by chemical cyclodehydration with acetic anhydride. However, cyano-substituted tetracarboxylic acid compound **2d** could not be obtained directly from **1d** due to the cyano group also being hydrolyzable to carboxylic acid. Alternatively, the Schmidt reaction[14] of aldehyde with NaN_3 and trifluoromethanesulfonic acid (TfOH) was used to obtain the corresponding nitrile compound **2d** with carboxylic acid groups on the TPA moiety, and **2d** then was converted to the dianhydride **3d** by cyclodehydration. Elemental analysis, ^{1}H NMR, ^{13}C NMR, and FT-IR spectroscopic techniques were used to identify the structures of these compounds as shown in Fig. S1–S12.† The results of all the spectroscopic analyses suggest the successful preparation of the target molecules.

The preparation of these PIs was carried out by one-pot (Scheme S4†) and two-step polycondensation (Scheme S5†) procedures. In the one-pot procedure, the dianhydrides (**3a**, **3b**, and **4d**) and various diamines were polymerized in *m*-cresol at 200 °C in the presence of isoquinoline. The resulting viscous polyimide solutions were then precipitated in methanol. However, the formyl group in dianhydride monomer **3c** also could react with the diamine monomer. In order to prevent the side reaction forming an azomethine linkage, a low-temperature reaction condition was used to prepare the poly(amic acid)s from **3c** and diamine monomers in the first step. The resulting poly(amic acid)s were subsequently converted to polyimides **III** *via* a chemical imidization process by adding pyridine and acetic anhydride in the second step.

The inherent viscosities and molecular weights of these polymers are summarized in Table S1.† Transparent and tough films of **IId**, **IIId**, and **IVd** (Fig. 1) were obtained *via* solution casting. ^{1}H NMR and FT-IR spectroscopic techniques were used to identify structures of the obtained polyimides, and the spectra agree well with the proposed molecular structures (Fig. S13 and S14†).

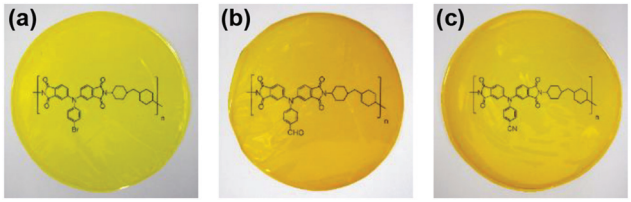

Fig. 1 The photographs of the polyimide materials, each with a thickness of about 30 μm. (a) **IId**, (b) **IIId**, and (c) **IVd**.

Basic polymer properties

The solubility behavior of these resulting PIs was investigated quantitatively at a concentration of 5 mg ml^{-1}, and the results are also listed in Table S2.† These PIs were readily soluble in low polarity solvents such as $CHCl_3$ and tetrahydrofuran (THF), and some highly polar aprotic organic solvents such as NMP and *m*-cresol. Thus, these TPA-containing PIs, when processed by spin-coating or inkjet printing, can be made to form high-performance thin films with the potential for practical applications.

Thermal properties of the obtained polymers were determined by thermogravimetric analysis (TGA) and differential scanning calorimetry (DSC), and the thermal behavior data are summarized in Table S3.† TGA curves of these PIs both in air and in a nitrogen atmosphere are shown in Fig. S15.† All the prepared PIs exhibited high thermal stability with insignificant weight loss up to 415 °C in air as well as in a nitrogen atmosphere. Typical DSC curves of resulting PIs with glass-transition temperatures (T_g) of 288–365 °C are depicted in Fig. S16.†

Optical properties of TPA luminogens

The optical properties of TPA luminogens in THF solutions were investigated by using UV-Vis and photoluminescence (PL) spectroscopy, which are depicted in Fig. 2 and summarized in Table S4.† PL photographs of TPA-containing luminogens in THF were taken under illumination at a wavelength of 365 nm as shown in Fig. S17.† Moreover, in order to gain more insight into the mechanism of luminescence, TD-DFT calculations were used to clarify the nature of the electron transitions of the target materials with different functional groups and substituents depicted in Fig. S18.† Diimide **1** and dianhydride **3** both showed two absorbance peaks, one at a wavelength range of about 225–300 nm and the other at 300–450 nm in a THF solution (concentration of **1** or **3**: 10 μM). The 225–300 nm absorption peak could be attributed to the high-energy level π–π* transition. The 300–450 nm peak involved two transitions, the LE π–π* and ICT π–π* transitions from the electron-donating TPA to the electron-accepting phthalic imide or phthalic anhydride, as a hybridized local and charge-transfer (HLCT) transition that exhibited a PL emission maximum at 471–518 nm. The rigid phthalic imide and phthalic anhydride groups with relatively extended conjugation appeared to have induced bathochromic shifts of the absorption and emission peaks while maintaining high intensities of these peaks both in the UV-Vis and PL spectra. Tetracarboxylic acid **2** also showed two broad absorbance peaks at about 225–275 nm and 275–400 nm attributed to relatively high-energy π–π* and HLCT transitions, respectively, and exhibited a PL emission maximum at 439–458 nm in the THF solution. The lower PLQYs and blue-shifted emissions of the compounds in the **2** series when compared with those in the **1** and **3** series could be attributed to the carboxylic acid groups. In addition, compounds of the **4** series, with its pristine TPA system, were also investigated for comparison. The TPA compounds **4** showed a main peak at around 300 nm ascribed to the LE π–π* transition, while **4c** and **4d** each showed additional absorption peaks, at about 353 nm and 324 nm, respectively, due to ICT from the central electron-donating TPA to the pendant electron-accepting substituents. Thus, the hybridized LE and ICT transition of **4c** and **4d** revealed emissions at 465 nm and 421 nm with high PLQY values of 36.0 and 28.5%, respectively.

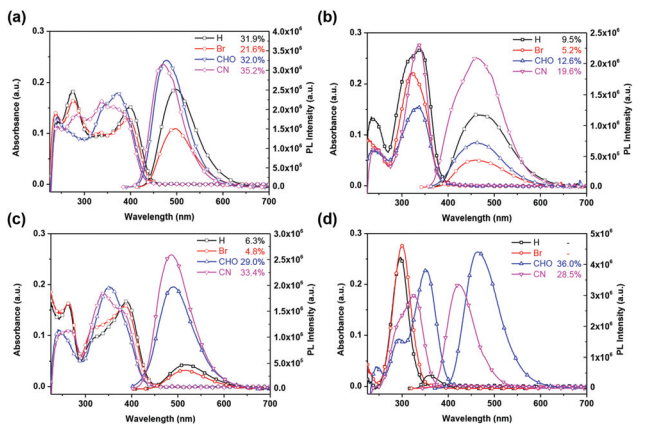

Fig. 2 Absorption and photoluminescence (PL) spectra of (a) diimides, (b) tetracarboxylic acids, (c) dianhydrides, and (d) TPA compounds in THF solutions (10 μM).

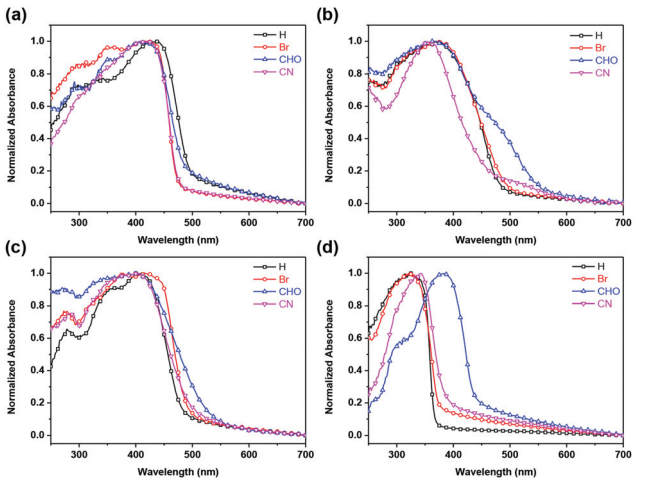

Fig. 3 Absorption spectra of (a) diimides, (b) tetracarboxylic acids, (c) dianhydrides, and (d) TPA compounds in the solid state.

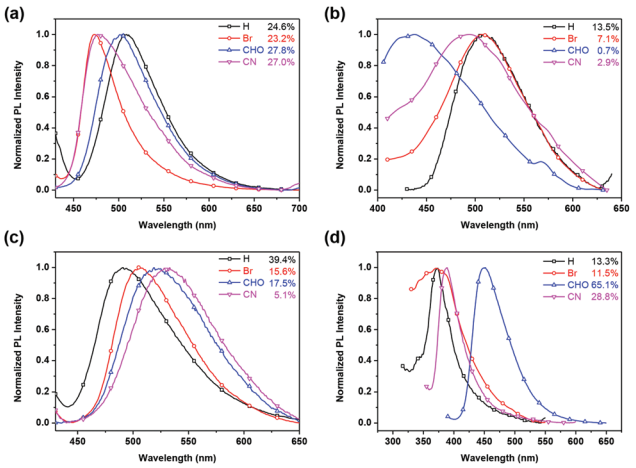

Fig. 4 Photoluminescence (PL) spectra of (a) diimides, (b) tetracarboxylic acids, (c) dianhydrides, and (d) TPA compounds in the solid state.

The optical properties of TPA-containing luminogens in the solid powder state were investigated by acquiring UV-Vis and PL spectra, which are shown in Fig. 3 and 4, respectively, and whose features are summarized in Table S4.† PL photographs of these compounds in the solid state were taken under illumination at a wavelength of 365 nm as shown in Fig. 5. The UV-Vis spectra of all series of luminogens revealed greater absorption peak widths and bathochromic shifts for the aggregated powder state than for the highly random solvated state due to intermolecular interactions in the former. The PL efficiency of the compounds of the **1** series exhibited similar values to those in THF solution state. The TPA-diimide luminogen showed AIEE behavior due to the rigid phthalic imide ring and propeller-like TPA, which restrict intramolecular motions in the solid state. The TPA-based luminogens of the **2** and **3** series with tetracarboxylic acid and dianhydride

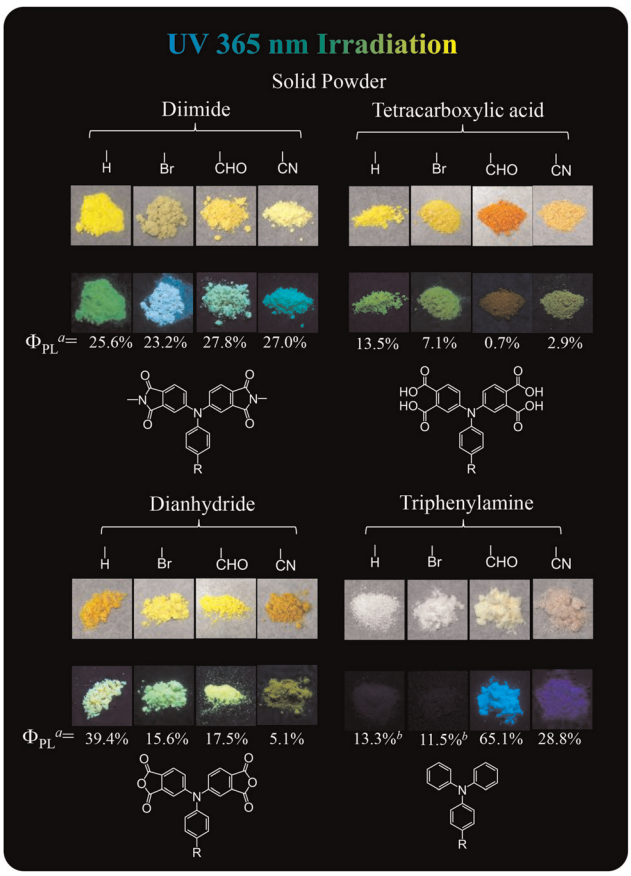

Fig. 5 Photographs of molecules in the solid powder state were taken under irradiation of 365 nm-wavelength UV light. ([a]The PL efficiency under illumination of λ_{max}^{abs} of the samples using calibrated integrating sphere; [b]Non-emission under irradiation of 365 nm-wavelength UV light due to a λ_{max}^{em} wavelength of about 371–373 nm.)

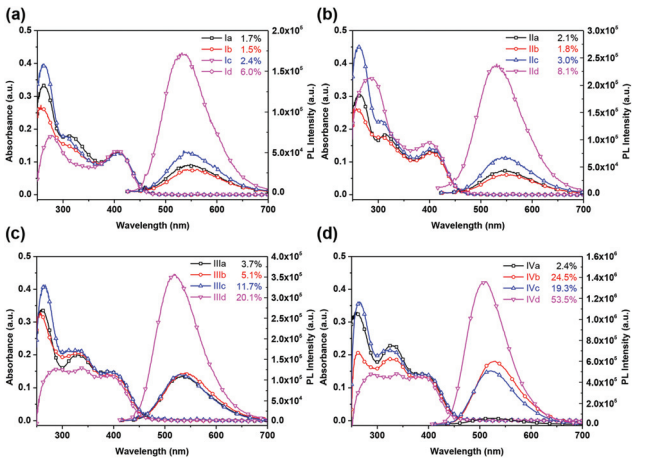

Fig. 6 Absorption and photoluminescence (PL) spectra of series of (a) **I**, (b) **II**, (c) **III**, and (d) **IV** polyimides in THF solutions (10 μM).

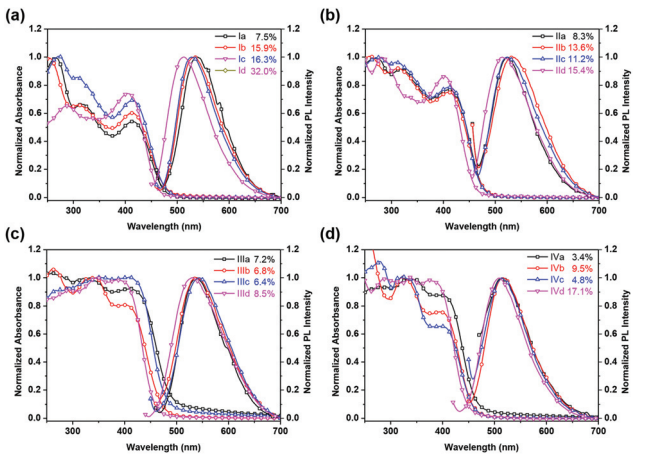

Fig. 7 Absorption and photoluminescence (PL) spectra of series of (a) **I**, (b) **II**, (c) **III**, and (d) **IV** polyimides in the solid film state.

functional groups revealed an opposite PL efficiency tendency between solution and solid states, especially for the cyano-containing **2d** and **3d**, which showed relatively low PLQYs, while **2a** and **3a** displayed the highest PLQYs in the solid powder state. Introducing electron acceptors into the TPA luminogens appeared to have facilitated HLCT absorption and hence enhanced the PLQY in the solution state. However, intermolecular CT absorption also increased in the aggregated state, and the overlapping of intermolecular CT absorption and emission bands resulted in a low PLQY.

Optical properties of polyimides

In the polymer system, the UV-Vis absorption and PL emission behaviors of the PIs in NMP solutions and in the solid film state are depicted in Fig. 6 and 7, respectively. The results are summarized in Table S5,† and PL photographs of the PIs in the film state are shown in Fig. 8 (solution state summarized in Fig. S19†). These PIs exhibited UV-Vis absorption bands at about 387–407 nm in the NMP solution due to HLCT π–π* transitions. Generally, the entirely aromatic polyimides (prepared from diamines **5a–c**), which have relatively extensive

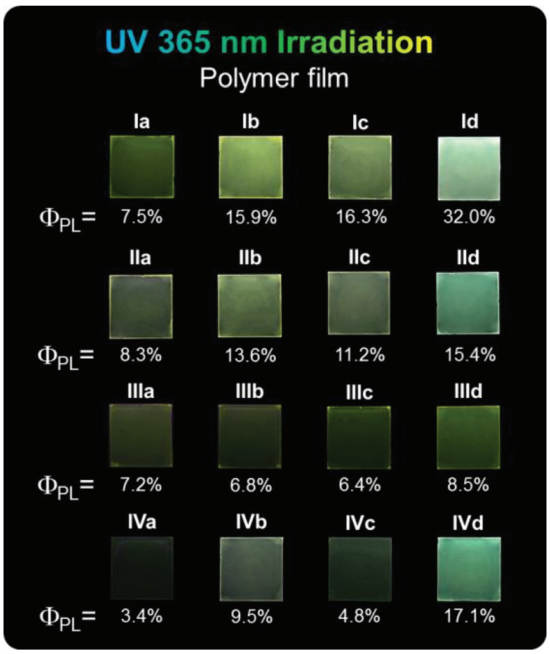

Fig. 8 Photographs of polyimides in the solid film state were taken under illumination of a 365 nm-wavelength UV light.

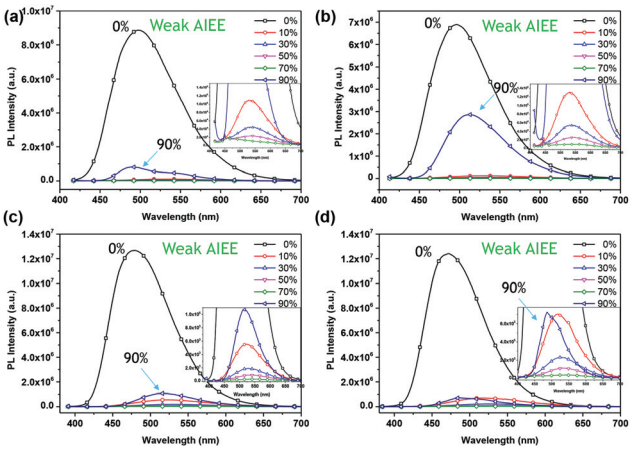

Fig. 9 PL spectra of diimide compounds in solutions with different THF-water fractions. (a) **1a**, (b) **1b**, (c) **1c**, and (d) **1d**.

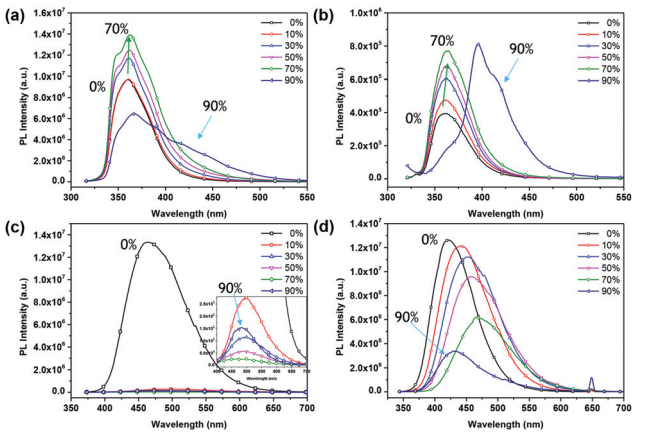

Fig. 10 PL spectra of triphenylamine compounds in solutions with different THF-water fractions. (a) **4a**, (b) **4b**, (c) **4c**, and (d) **4d**.

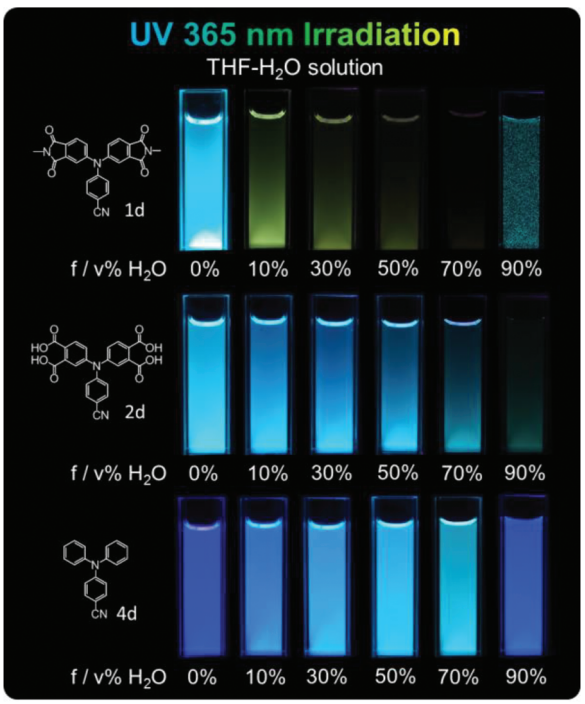

Fig. 11 Photographs of molecules in solutions with different THF-water fraction were taken under illumination of 365 nm-wavelength UV light.

intermolecular π–π interactions, displayed lower PLQYs than did the semi-aromatic polyimides (prepared from diamine **5d**). In the **I** and **II** series, the PL efficiency values of the PIs in the solid film state were higher than those in the NMP solution state, and the emission peaks revealed hypsochromic shifts relative to those of the PI solutions. This phenomenon could be attributed to the AIEE effects resulting from the introduction of the rigid phthalic imide and propeller-like TPA moieties that we have described in the previous study.[13] In contrast, the **III** and **IV** series showed higher PL efficiency values in the NMP solution than did the **I** and **II** series; **IIId** and **IVd** showed especially high PL efficiency values, with PLQYs of 20.1% and 53.5%, respectively. However, in the film state, the PLQYs of **III** and **IV** were observed to be similar to those of the **I** and **II** series. The HLCT transition could be enhanced by introducing the electron acceptor into the TPA luminogens to exhibit higher PLQY in the solution state, but also facilitated intermolecular charge transfer and energy transfer interactions in solid film state which led to ACQ effect and resulted in lower PLQY.

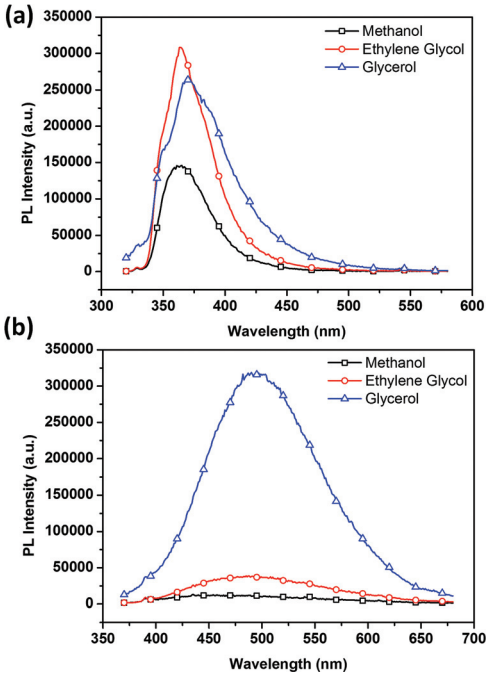

Fig. 12 PL spectra of (a) **4b** and (b) **4c** in methanol, ethylene glycol and glycerol.

AIEE effect

Absorption and PL emission spectra of TPA luminogens of the **1** and **4** series in THF solutions with different water fractions were used to investigate the aggregation effect on PL intensity as depicted in Fig. S20, 9, S21,† and 10. Typical PL photographs such as those of **1d**, **2d**, and **4d** are shown in Fig. 11 (the solvent effects of **4b** and **4c** are shown in Fig. S22†). The TPA luminogens of the **1** and **4** series are highly soluble in THF and insoluble in water. Therefore, increasing the water fraction in the THF-water mixture could promote the formation of aggregated luminogen particles rather than the sol-

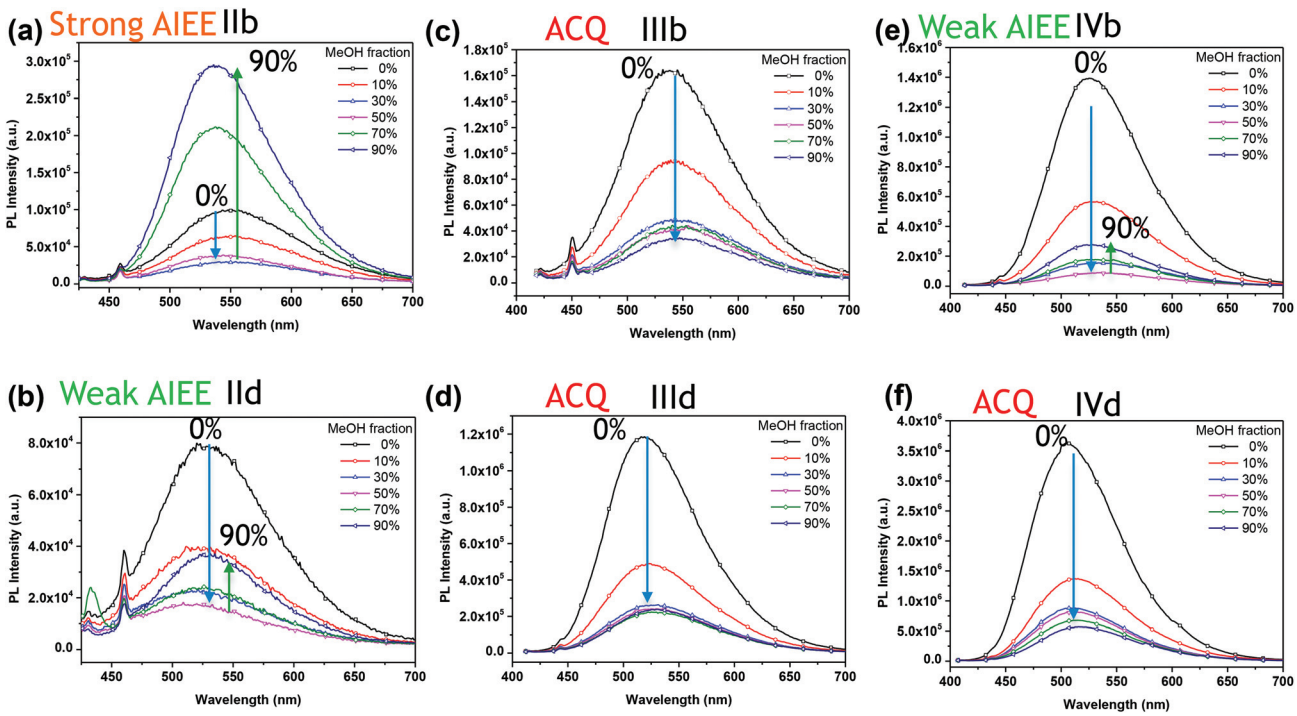

Fig. 13 PL spectra of polyimides in solutions with different NMP-MeOH fractions. (a) **IIb**, (b) **IId**, (c) **IIb**, (d) **IIId**, (e) **IVb**, and (f) **IVd**.

vated state and hence change the absorption and fluorescence properties of the luminogens. For example, the diimide luminogen **Id** (Fig. 9d) in a pure THF solution exhibited a blue PL emission with a maximum peak at about 471 nm, while the PL emission was obviously red-shifted to green, and the PL intensity was also reduced upon increasing the water fraction from 10 to 70 vol%.

Generally, the fluorescence behaviors of D–A luminogens were highly sensitive to solvent polarity, and the reduction of the PL intensity could be attributed to the solvent effect caused by the high polarity of water. Furthermore, when the water fraction was increased to 90 vol% or more, the emission was blue-shifted back again, and with an enhanced intensity at the same time, which could be attributed to molecular aggregation, and the restriction of intramolecular motions resulted in higher PL intensities than displayed by the low water fractions. A similar phenomenon was observed in the cases of TPA luminogens **4c** and **4d**. In addition, the PL intensities of **4a** and **4b** were enhanced and red-shifted when the water fraction was increased from 10% to 70%. A shoulder appeared at a wavelength of about 425 nm for **4a** and a new peak at about 400 nm for **4b** when the water fraction was 90%. This phenomenon could be due to enhanced CT transition emissions with increased solvent polarity[15] and aggregation of the molecules. Furthermore, the effect of solvent viscosity on the emission behavior was also investigated and demonstrated. The viscosity of glycerol at 25 °C was observed to be 934 cp, about 720 times greater than that of methanol (0.544 cp).[16] The PL intensities of **4b** and **4c** in glycerol solution were, respectively, 1.7 and 25-fold higher than that in the methanol solution (Fig. 12).

For the polyimides, the PL emission behaviors of the entirely aromatic (prepared from diamine **5b**) and semi-aromatic (prepared from diamine **5d**) polyimides in diluted NMP-methanol mixtures with different methanol fractions were used to investigate the effect of aggregation on PL intensity as shown in Fig. 13; representative PL photographs are shown in Fig. 14. When methanol was added to **IIb**, the emission was dramatically weakened, and the emission recovered by increasing the methanol fraction to 70%, and could be intensified and blue-shifted with further increases in methanol fractions. **IVb** revealed a similar phenomenon of reduced PL intensity upon increasing the methanol fraction from 0 to 50%. The emission intensity of **IVb** was enhanced upon increasing the methanol fraction from 50 to 70%, but did not return to original state when the methanol fraction was increased to 90%. The semi-aromatic TPA-containing PIs exhibited weak AIEE or ACQ activity, maybe due to the configuration of cyclohexane and soft methylene segments although they showed higher PL efficiency values than did the completely aromatic PIs. However, **IIIb**, **IIId** and **IVd** showed only ACQ behavior.

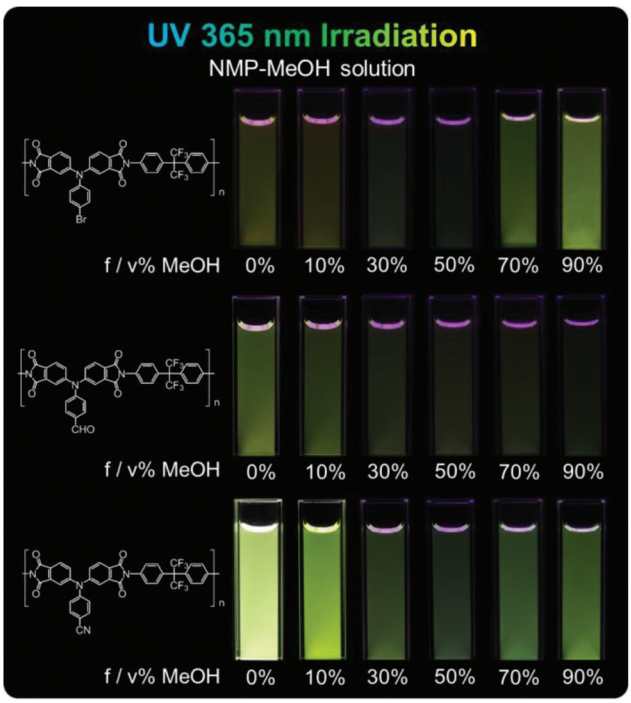

Fig. 14 Photographs of polyimides in solutions with different NMP-MeOH fractions were taken under illumination of 365 nm-wavelength UV light.

Conclusions

We prepared four series of TPA-based luminogens with various functional groups (diphthalic imide, tetracarboxylic acid, diphthalic anhydride, and pristine TPA) and substituents (–H, –Br, –CHO, and –CN). The corresponding fluorescent PIs derived from TPA-based dianhydride monomers with aromatic and aliphatic diamine monomers were also successfully prepared. In the solution state, the introduction of strong electron acceptors such as formyl and cyano substituents in the luminogens induced strong emissions due to hybridized local and charge-transfer transitions. However, aggregated molecules containing these pendant electron-accepting groups resulted in a quenching fluorescence behavior due to intermolecular interactions and energy transfers. The competition of AIEE and ACQ effects was observed in PL spectra both of small molecules and polyimides in the solution state with various fractions of poor solvent. We expect the current comparative study of functional groups and substituent effects on TPA-based luminogens to provide clues for designing new high-efficiency AIE-active luminogens and photoluminescent PIs.

Acknowledgements

The authors gratefully acknowledge the Ministry of Science and Technology of Taiwan for financial support, and C.-W. Lu and S.-L. Huang in the Instrumentation Center of National Taiwan University for assistance with CHNS elemental analysis (EA) and nuclear magnetic resonance (NMR) experiments, respectively.

Notes and references

1 (*a*) J. Wu, W. Liu, J. Ge, H. Zhang and P. Wang, *Chem. Soc. Rev.*, 2011, **40**, 3483; (*b*) H. N. Kim, Z. Guo, W. Zhu, J. Yoon and H. Tian, *Chem. Soc. Rev.*, 2011, **40**, 79; (*c*) R. T. Kwok, C. W. Leung, J. W. Lam and B. Z. Tang, *Chem. Soc. Rev.*, 2015, **44**, 4228; (*d*) S. M. Borisov and O. S. Wolfbeis, *Chem. Rev.*, 2008, **108**, 423.

2 (*a*) Y. Yang, Q. Zhao, W. Feng and F. Li, *Chem. Rev.*, 2013, **113**, 192; (*b*) H. Mattoussi, G. Palui and H. B. Na, *Adv. Drug Delivery Rev.*, 2012, **64**, 138.

3 (*a*) H. Yersin, *Highly Efficient OLEDs with Phosphorescent Materials*, Wiley-VCH, Weinheim, 2008; (*b*) M. C. Gather, A. Kohnen and K. Meerholz, *Adv. Mater.*, 2011, **23**, 233.

4 (*a*) I. D. W. Samuel and G. A. Turnbull, *Chem. Rev.*, 2007, **107**, 1272; (*b*) L. Persano, A. Camposeo and D. Pisignano, *Prog. Polym. Sci.*, 2015, **43**, 48; (*c*) H. Wang, E. G. Zhao, J. W. Y. Lam and B. Z. Tang, *Mater. Today*, 2015, **18**, 365.

5 J. D. Luo, Z. L. Xie, J. W. Y. Lam, L. Cheng, H. Y. Chen, C. F. Qiu, H. S. Kwok, X. W. Zhan, Y. Q. Liu, D. B. Zhu and B. Z. Tang, *Chem. Commun.*, 2001, 1740.

6 (*a*) J. Mei, Y. Hong, J. W. Y. Lam, A. Qin, Y. Tang and B. Z. Tang, *Adv. Mater.*, 2014, **26**, 5429; (*b*) R. Hu, N. L. C. Leung and B. Z. Tang, *Chem. Soc. Rev.*, 2014, **43**, 4494.

7 (*a*) A. Eisfeld and J. S. Briggs, *Chem. Phys.*, 2006, **324**, 376; (*b*) F. Wuerthner, T. E. Kaiser and C. R. Saha-Moeller, *Angew. Chem., Int. Ed.*, 2011, **50**, 3376; (*c*) Y. Wang, T. Liu, L. Bu, J. Li, C. Yang, X. Li, Y. Tao and W. Yang, *J. Phys. Chem. C*, 2012, **116**, 15576; (*d*) B. K. An, S. K. Kwon, S. D. Jung and S. Y. Park, *J. Am. Chem. Soc.*, 2002, **124**, 14410.

8 (*a*) Y. Hong, J. W. Y. Lam and B. Z. Tang, *Chem. Commun.*, 2009, 4332; (*b*) Y. Hong, J. W. Y. Lam and B. Z. Tang, *Chem. Soc. Rev.*, 2011, **40**, 5361; (*c*) Z. Q. Yan, Z. Y. Yang, H. Wang, A. W. Li, L. P. Wang, H. Yang and B. R. Gao, *Spectrochim. Acta, Part A*, 2011, **78**, 1640; (*d*) H. H. Fang, Q. D. Chen, J. Yang, H. Xia, B. R. Gao, J. Feng, Y. G. Ma and H. B. Sun, *J. Phys. Chem. C*, 2010, **114**, 11958; (*e*) R. Hu, E. Lager, A. Aguilar-Aguilar, J. Liu, J. W. Y. Lam, H. H. Y. Sung, I. D. Williams, Y. Zhong, K. S. Wong, E. Pena-Cabrera and B. Z. Tang, *J. Phys. Chem. C*, 2009, **113**, 15845; (*f*) W. Qin, D. Ding, J. Liu, W. Z. Yuan, Y. Hu, B. Liu and B. Z. Tang, *Adv. Funct. Mater.*, 2012, **22**, 771.

9 (*a*) T. Mutai, H. Sawatani, T. Shida, H. Shono and K. Araki, *J. Org. Chem.*, 2013, **78**, 2482; (*b*) Y. Shigemitsu, T. Mutai, H. Houjou and K. Araki, *J. Phys. Chem. A*, 2012, **116**, 12041; (*c*) R. Wei, P. Song and A. Tong, *J. Phys. Chem. C*, 2013, **117**, 3467.

10 (*a*) J. W. Chen, C. C. W. Law, J. W. Y. Lam, Y. P. Dong, S. M. F. Lo, I. D. Williams, D. B. Zhu and B. Z. Tang, *Chem. Mater.*, 2003, **15**, 1535; (*b*) J. Luo, K. Song, F. L. Gu and Q. Miao, *Chem. Sci.*, 2011, **2**, 2029.

11 (*a*) A. Iwan and D. Sek, *Prog. Polym. Sci.*, 2011, **36**, 1277; (*b*) J. H. Wu and G. S. Liou, *Adv. Funct. Mater.*, 2014, **24**, 6422; (*c*) H. J. Yen and G. S. Liou, *Polym. J.*, 2015, DOI: 10.1038/pj.2015.87.

12 W. Li, Y. Pan, L. Yao, H. Liu, S. Zhang, C. Wang, F. Shen, P. Lu, B. Yang and Y. Ma, *Adv. Opt. Mater.*, 2014, **2**, 892.

13 (*a*) J. H. Wu and G. S. Liou, *Polym. Chem.*, 2015, **6**, 5225; (*b*) H. J. Yen, J. H. Wu, W. C. Wang and G. S. Liou, *Adv. Opt. Mater.*, 2013, **1**, 668.

14 B. V. Rokade and K. R. Prabhu, *J. Org. Chem.*, 2012, **77**, 5364.

15 W. Schuddeboom, S. A. Jonker, J. M. Warman, U. Leinhos, W. Kuehnle and K. A. Zachariasse, *J. Chem. Phys. Chem.*, 1992, **96**, 10809.

16 *CRC Handbook of Chemistry and Physics*, ed. W. M. Haynes, CRC Press/Taylor and Francis, Boca Raton, FL, 96th edn, 2015.

